HEFAT2012
9th International Conference on Heat Transfer, Fluid Mechanics and Thermodynamics
16 – 18 July 2012
Malta

DRAG REDUCTION OF CYLINDERS BY PARTIAL POROUS COATING

Ruck, B.*, Klausmann, K. and Wacker, T.
*Author for correspondence
Laboratory of Building- and Environmental Aerodynamics, IfH
Karlsruhe Institute of Technology KIT, Karlsruhe, 76131, Germany
E-mail: ruck@kit.edu

ABSTRACT

The paper summarizes experimental investigations concerning drag reduction of circular cylinders by porous coating. In order to quantify the effect, wind tunnel experiments with a force balance and flow field analyses have been carried out.

In a first experiment, the cylinders were coated completely with a thin porous layer. The results show that the boundary layer over the porous surface is turbulent right from the beginning and thickens faster because of the enhanced vertical momentum exchange when compared to a smooth cylinder surface. The region of flow detachment is widened resulting in a broader area with almost vanishing low flow velocities. All in all, the measurements show that a full porous coating of the cylinders increase the flow resistance.

In a second experiment, the cylinders were coated only on the leeward side, which resulted in a reduction of the body's flow resistance. This effect seems due to the fact that the recirculating velocity and the underpressure in the wake is reduced significantly through a leeward porous coating. Thus, combining a smooth non-permeable windward side with a porously coated leeward side can lead to a drag reduction of the body. These findings can be applied advantageously in many technical areas, such as energy saving of moving bodies (cars/trains/planes) or in reducing fluid loads on submersed bodies.

INTRODUCTION

In the past, fluid mechanical research in the field of porous, permeable media has been centered mainly on low porosities. Typically, Darcy's law (Darcy 1856 [1], Bear 1972 [2]) and the Darcy-Forchheimer law (Forchheimer 1914-1916 [3]) were used to describe flow and pressure losses. The validity of these laws are limited and they cannot be applied when the flow velocities are no longer small and the pore volume of the porous medium is so large (pore volume / total volume > 95%) that turbulence can be sustained in the pores or even generated. The flow through high-porous media as well as the boundary layer characteristics of flows along high-porous permeable surfaces has not been examined sufficiently so far. In this area, there is a lack of knowledge even for flows around simple geometries i.e. flow around circular cylinders or spheres with highly porous surface coating.

First numerical simulations (DNS) on flows over high-porous surfaces exist, however, at very low Reynolds numbers, see e.g. Breugem et al. 2006 [4]. These simulations suggest that quantitative and qualitative differences exist in the boundary layer flow over smooth/rough and porous/permeable walls. Turbulence near permeable walls comprises vortex structures of larger scale, including those originating from Kelvin-Helmholtz instabilities.

On the issue of flow over porous permeable walls, there are few studies that indicate that one could use the interfacial effects advantageously in drag reduction. Coating surfaces with porous materials could be energy-saving as stated by Bruneau et al. 2006 [5], who found in a numerical simulation that the resistance of vehicles could be reduced up to 45%. The reason for this might be an increase in base pressure in the lee of the vehicle induced by thin porous layers attached to the rear part of the vehicle. Other numerical simulations indicated that the amplitude of vortex shedding, which can lead to destructive structure oscillations, can be reduced by applying a porous outer layer (sheath) on the component (Bruneau et al. 2006 [6], see also Bhattascharyya et al. 2011 [7]). It should be noted, that there are currently only few studies on the topic of flow around porously coated bluff bodies and that the basic knowledge in this field has not been elaborated so far.

Since the few existing studies are mainly of numerical type and subject to well-know limitations (DNS only at very low Reynolds numbers; subgrid scale modelling of LES cannot predict real interfacial flow phenomena; wall functions of k-ε models cannot resolve correctly flow physics at surfaces / interfaces), experimental investigations are lacking, which contribute to the fundamental understanding of the phenomena involved.

CYLINDER FLOW AND ROUGHNESS

The study of flow and resistance of smooth circular cylinders is connected historically with the names of Strouhal 1878 [8], von Kármán 1911 [9], Wieselsberger 1921 [10] and Roshko 1961 [11]. A good summary of fundamental results of different authors can be found in Hoerner 1965 [12] and in Zdravkovich 1997 and 2003 [13,14]. Rough cylinders were investigated in particular by Fage and Warsap 1929 [15], Achenbach 1968 and 1971 [16,17], and Achenbach and Heinecke 1981 [18]. The contributions of these authors are well know, however, their findings are limited to smooth and rough cylinders, which is of course different from cylinders with porous coatings.

Nikuradse 1933 [19] introduced the term of 'sand roughness' in order to compare rough surfaces. Sand roughness describes the height k_s of a layer of sand grains of one single diameter, which were tightly and homogeneously packed on the surface of a body. Technical surfaces, however, have often no such uniformity of roughness elements. They show irregularities and textures, so that the concept of equivalent sand roughness k_{se} had to be introduced. This concept describes the roughness of the real complex surface as being generated by a constant sand roughness of tightly and homogeneously packed sand grains on the surface, which induces the same fluid mechanical effect as the real complex surface. The roughness of a surface is classified in fluid mechanics by a roughness Reynolds number Re_k. It represents the ratio of sand roughness to viscous length L (a measure of the thickness of the viscous sublayer) so that $Re_k = k_s / L$. For $Re_k < 5$, the surface is hydraulically smooth and the roughness elements are covered by the viscous sublayer. The range $5 < Re_k < 70$ is referred to as the transitional range and $Re_k > 70$ characterizes a fully rough surface, where the roughness elements on the wall protrude into the zone of the validity of the logarithmic law of the wall.

These definitions and determinations, however, are not comprehensive enough to characterize fully rugged and permeable walls. Wall roughness and wall permeability are not the same and induce from a phenomenological point of view different flow behaviour. This was already found by Price 1956 [20] and Wong 1979 [21], who reported about a delay in vortex formation and about a suppression of vibration of shrouded cylindrical pillars realized by slats. According to Price 1956 [20], the mechanism of vibration suppression is induced by the delay in vortex street formation. The latter can be seen clearly in the visualization study of Galbraith 1980 [22], who analysed the flow pattern around a shrouded cylinder at $Re = 5*10^3$ and who reported about a significant base bleed. He concluded that the greater the amount of base bleed the longer the vortices take to form and the lower the drag. This seems to hold not only for permeable shrouds, but also for high-porous permeable homogeneous surface layers as they are presented in this paper.

Using high-porous and permeable media for coating of surfaces, the surface elements of the material act as small individual bluff bodies submerged in a flow, so that pressure distributions around these multiple elements build up. Thus, in contrary to the flow along a flat smooth or rough plate, the drag induced by the flow along the high-porous permeable interface consists of friction and pressure components.

Characteristically, the boundary layer at a high-porous interface shows transverse fluctuations, which can penetrate into the high-porous medium (momentum in flow direction, which is transported in transverse direction). As a consequence, additional drag is induced, which increase the flow losses. Thus, the flow along a high-porous interface can no longer be described as a simple flow along a smooth or sand rough wall, where no transverse fluctuations occur.

EXPERIMENTAL DETAILS

TEST CYLINDERS

In order to measure the fluid mechanical effect of high-porous coating, cylinders were made of balsa wood cores. The length was for all cylinders L = 70 cm. The wood core was encased in the different series of experiments with a high-porous shell. The outer diameter remained for all cylinders constant with D = 70 mm. The porous coating of the cylinder was made of the technical Poret foam-Ester from EMW Filtration GmbH, 65582 Diez, Germany. Poret-Ester foam is conventional polyester foam with high toughness and sponge-like porosity available in a wide range of sizes and shapes and wide-spread in engineering. The used foam varied according to the layer thickness and the chosen porosity. Three different layer thicknesses were tested dM = 10 mm, dM = 5 mm and dM = 3 mm. The porosity depending on the number of pores per inch was varied three times with ppi-values of 10, 20 and 30, see Figure 1. Figure 2 shows several fully jacketed cylinders.

Figure 1 Poret Ester foam with different permeability; thickness 5 mm

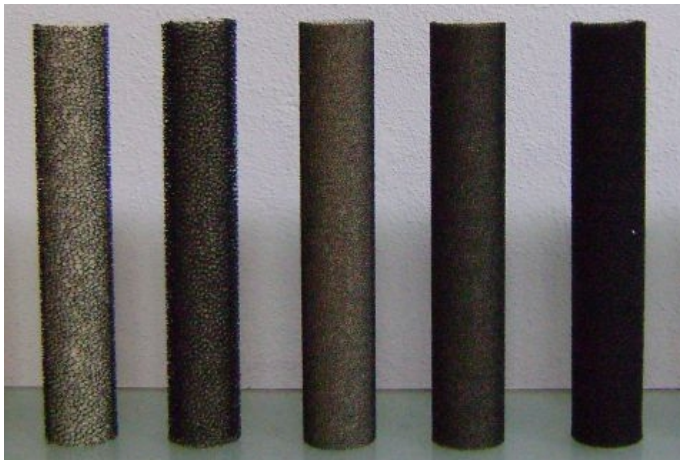

Figure 2 Photo of investigated, fully jacketed cylinders

By separate pressure drop measurements in a small close-loop wind tunnel, the loss coefficients of the technical foams were determined. For the large-pore foam (10 ppi) a pressure loss coefficient of $\lambda \approx 250$ was measured. The pressure loss coefficients for the 20 ppi foam and the 30 ppi foam were $\lambda \approx 500$ and $\lambda \approx 1000$ respectively.

For a second measurement series, eight circular cylinders were built with remaining constant outer diameter. Pore size and thickness of the permeable material remained also the same. The cylinders differ from the first series of experiments by the fact that the individual cylinders were not completely covered by the high-porous medium, but only the leeward side, as can be inferred from Fig. 3. For both experimental series, infinitely long cylinders were simulated using splitter plates at their ends. In Fig. 4 and 5, all types of investigated cylinders are listed.

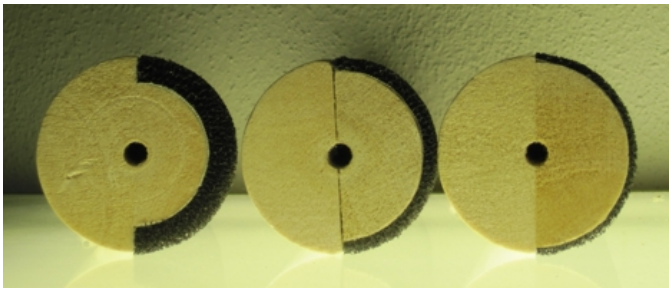

Figure 3 Photo of the test cylinders coated with high-porous foams and varying layer thickness on the leeward side

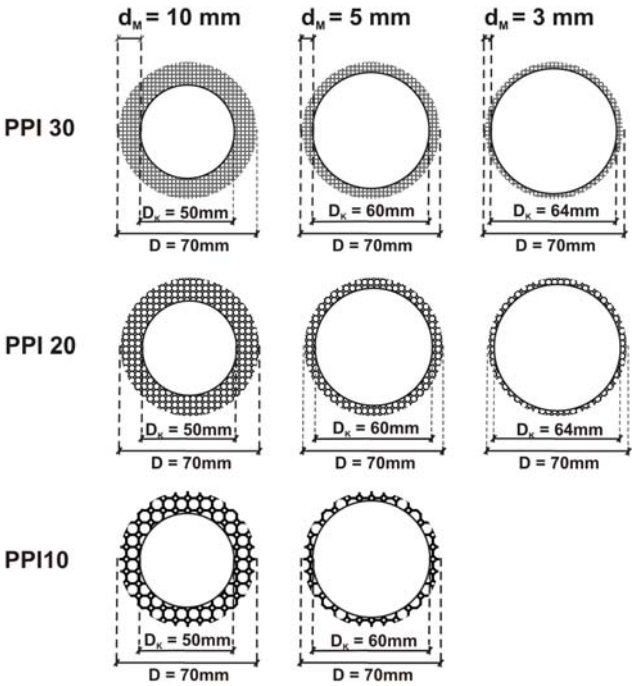

Figure 4 Investigated configurations of fully coated cylinders with porous media of different permeability and thickness

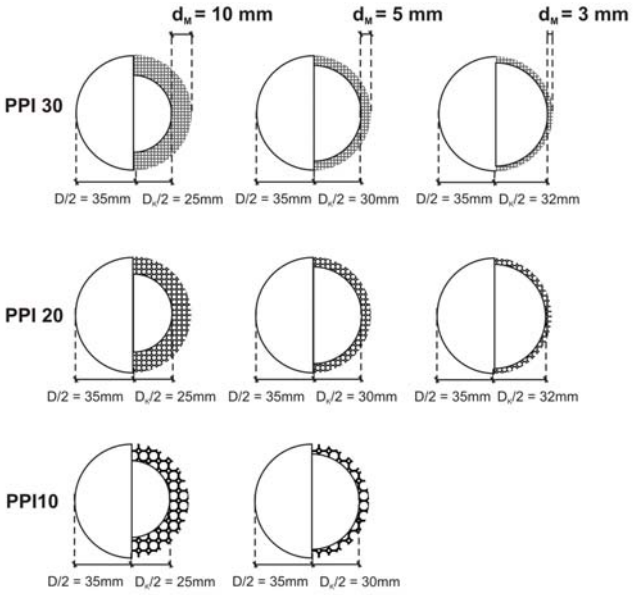

Figure 5 Investigated configurations of partially coated cylinders (lee) with porous media of different permeability and Thickness, see also Figure 3

DRAG MEASUREMENTS

To measure the flow resistance of porous-coated cylinders in the wind tunnel experiment, a force balance was used, see Fig. 6 and 7. For both experimental series, the Reynolds number was systematically varied in the range from 10^4 to $1.3*10^5$. In each series, a completely smooth (varnished) cylinder was measured as reference case.

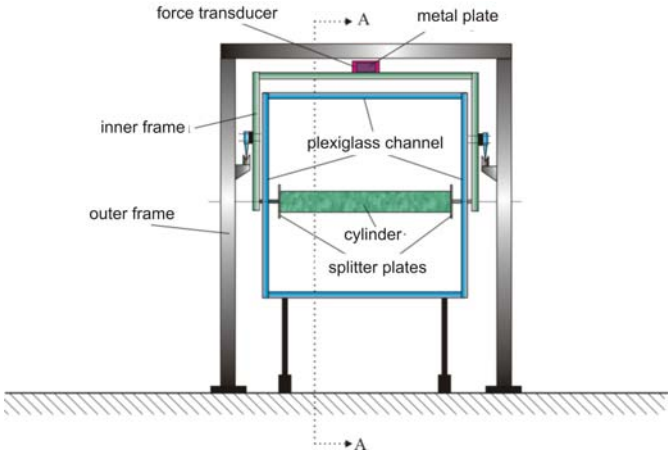

Figure 6 Force balance built in wind tunnel; view in streamwise direction

QUANTITATIVE AND QUALITATIVE FLOW ANALYSIS

For the quantitative analysis of the velocity field in the wake of the cylinders a 2D LDA system was applied, which delivered at each measuring point the horizontal and the vertical component of the velocity vector simultaneously. As laser light source a 4 Watt argon ion continuous wave laser Innova 90 was used with the wavelengths $\lambda 1 = 514.5$ nm (green) and

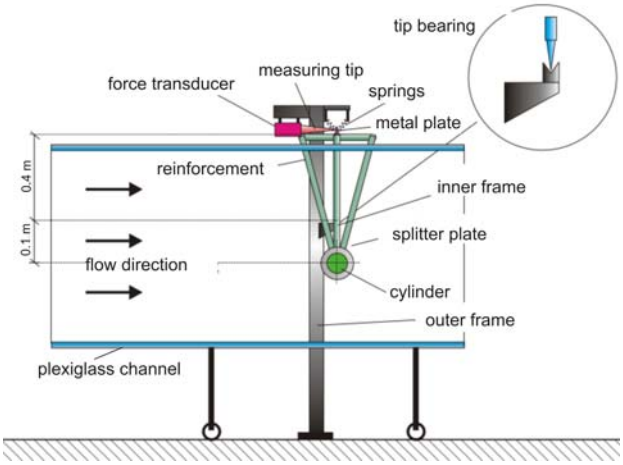

Figure 7 Side view of experimental set-up with force balance

λ2 = 488.0 nm (blue). The four partial laser beams for realizing the 2D LDA principle were guided by fiber optical waveguides to the measuring head (focal length 700 mm). For the investigations, the air was seeded with 1.2 - propylene glycol droplets having a diameter of 1-3 microns. Figure 8 shows the intersecting laser beams behind a measuring cylinder in the wind tunnel. The signal analysis was performed with a digital burst correlator made by TSI model IFA 750.

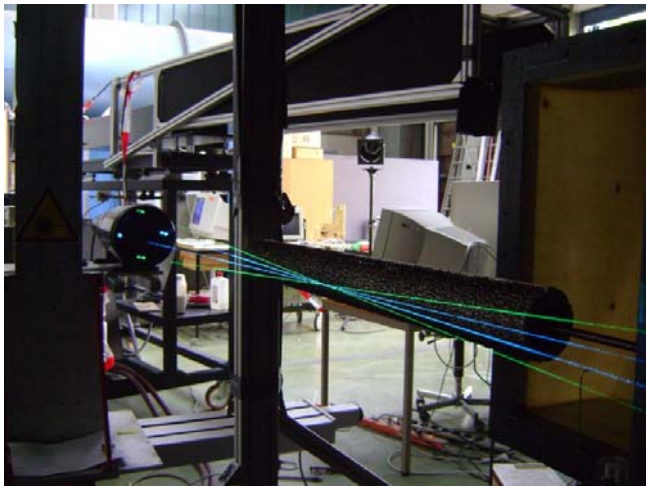

Figure 8 2D laser Doppler anemometry to measure the flow field in the wake of porous-coated cylinders

Downstream of the cylinders, a velocity field of size 28 cm x 42 cm was measured. In this field, the measurements were performed along nine vertical lines, each with 29 measurement positions, which have a vertical spacing of 1 cm. The first vertical measuring line was laid at a distance of x / d = 0.4 from the cylinder outer edge. The last line was positioned at x / d = 6. All in all, 261 data points were measured for each cylinder at a fixed Reynolds number of Re = 12,000.

For the qualitative analysis, the flow field was visualized by laser light sheet technique and dense seeding. The image detection was performed with a high-speed camera type PCO 1200HS. The camera can realize frame rates of 636 fps at full resolution of 1280 x 1024 pixels. It has an internal memory of 4 gigabytes and allows high data rates of up to 1 Gigabyte/sec. For the generation of laser light sheets at high repetition rate two Nd:YAG lasers from LEE were used working in pulse mode (maximum lamp power 6 kW, Q-switched operation 10 kHz with an average power of 44.9 W for laser 1 and 48.8 W for laser 2).

All measurements, i.e. drag measurements and quantitative as well as qualitative flow analyses, were performed in a closed-return wind tunnel with open test section (Göttinger type) with a length of 12.6 m, in which speeds of up to 50 m/s can be realized. The cross section of the nozzle is 75 cm x 75 cm and the test section has a length of 3.30 m. Measured shortly behind the nozzle outlet (distance 22 mm), the turbulent intensity is about 2%. The measurements of the cylinders were performed at a distance of 61.5 cm behind the nozzle outlet, so that it could be ensured that the entire experimental arrangement was exposed to the uniform flow core of the nozzle.

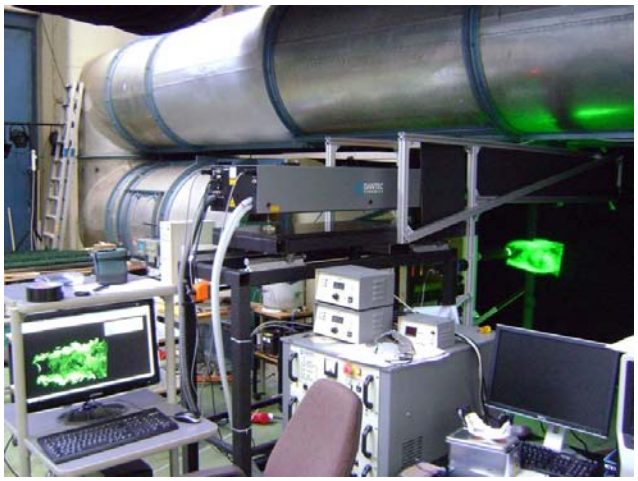

Figure 9 Laser light sheet technique applied in the wind tunnel for qualitative flow analyses

RESULTS

The boundary layer of the fully rough, high-porous and permeable interface is turbulent from the beginning. The porous 'roughness' produces small-scale turbulence and turbulent fluctuations occur along and through the permeable interface. Particularly because of the vertical momentum exchange, the boundary layer along the interface thickens quickly resulting in higher losses and in higher total resistance when compared to a smooth wall.

In Figure 10, the increase in drag coefficient of the cylinders with different porosities of the coating can be seen. It can be inferred that the drag of the smooth (varnished) cylinder is lowest and that, apparently, there is no linear relationship bet-

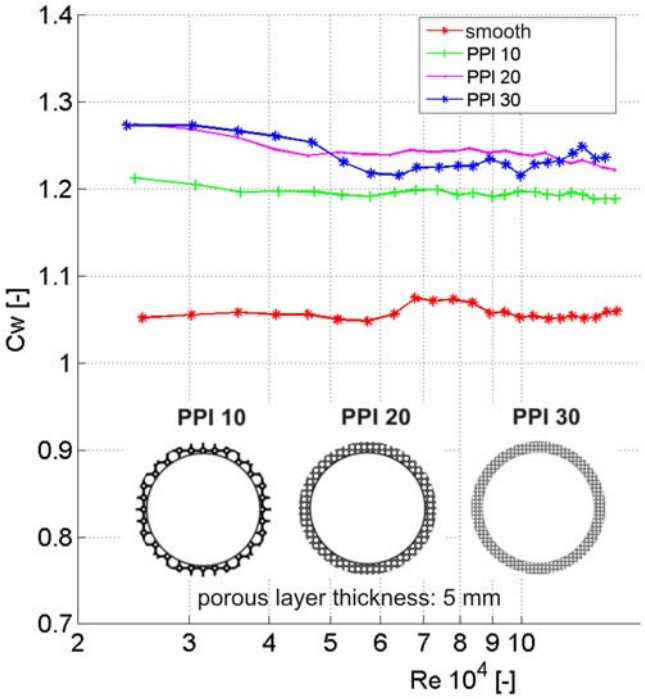

Figure 10 Drag coefficients for cylinders with coatings of different porosity; thickness of porous layer 5 mm

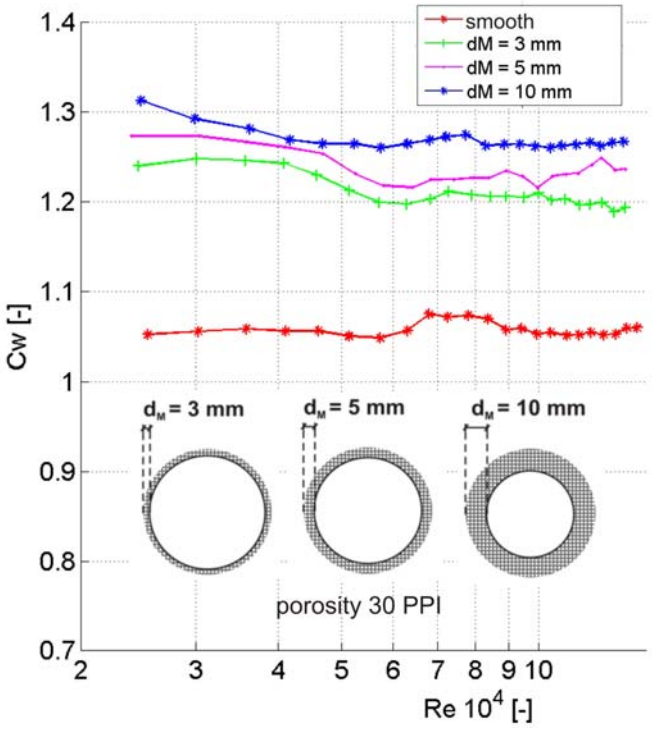

Figure 11 Drag coefficients for cylinders with coatings of fixed porosity (30 PPI) and varying thickness of porous layer

ween drag and porosity. On the other hand, the drag coefficients seem to be quite constant in the investigated range of Reynolds numbers. The drag coefficients of the fully coated cylinders are 15-25% higher than for the smooth cylinder. In Figure 11, the drag coefficients for coatings with a fixed permeability (30 ppi) but varying thickness are shown. Obviously, the drag increases with increasing layer thickness. Whereas for all configurations of fully porous-coated cylinders the drag coefficient increases when compared to the smooth cylinder, the situation changes with selective coating on the leeward side only. In fact, the drag coefficients decrease below the values of the smooth cylinder, see Figure 12.

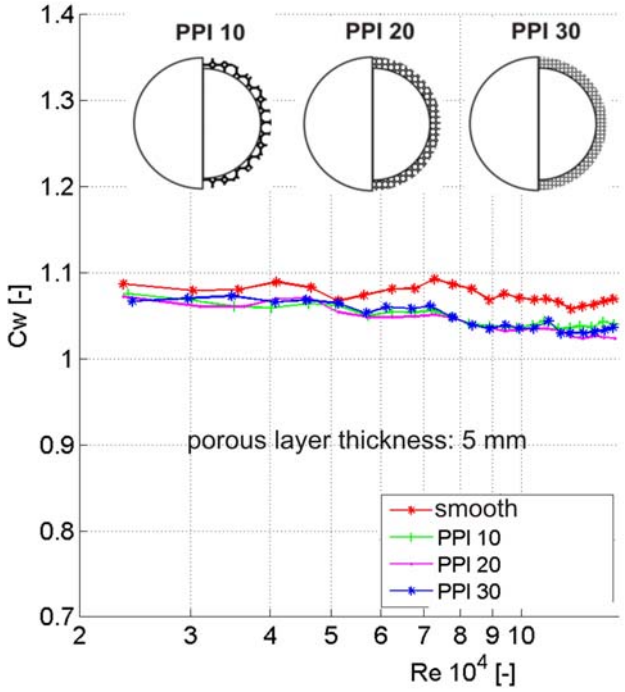

Figure 12 Drag coefficients for cylinders with coatings of different porosity in the lee; thickness of porous layer 5 mm

Flow analysis by laser Doppler anemometry reveals that the velocity profiles in the wake for smooth and fully coated cylinders differ from each other. As can be inferred from Figure 13 and 14 for a porous layer thickness of 10 mm and a porosity of 30 ppi, the wake is wider for the fully coated cylinder. Apparently, the recirculating flow velocity in the wake is reduced up to 40%. The span of measured velocities, e.g. on the horizontal center line between the near and far field of the fully coated cylinder, is reduced when compared to the smooth cylinder. This is a strong indication that the base pressure in the lee is increased (underpressure is decreased), which seems to be the reason for the overall drag reduction of the body.

The profiles of the turbulent kinetic energy (TKE) along the a vertical measurement line at x / d = 1.0 close to the cylinder, see Figure 15, show that with increasing porosity of the coating, the TKE is reduced and the shear layer becomes smaller.

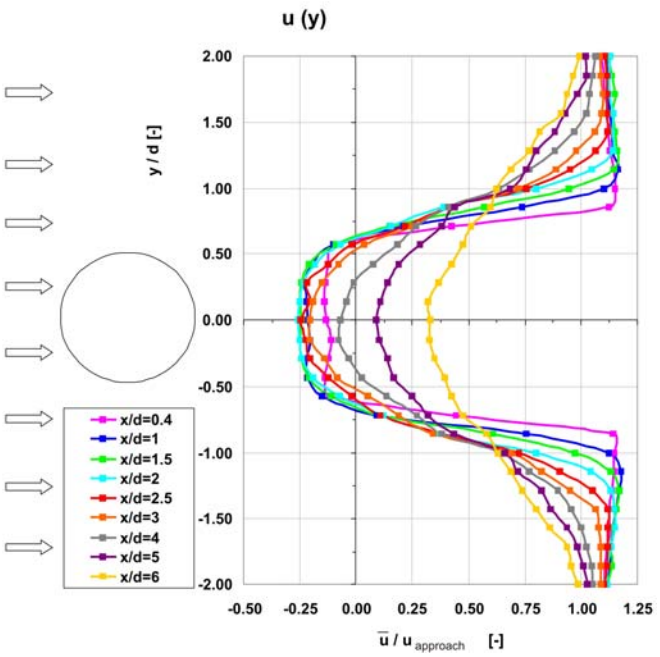

Figure 13 Profiles of horizontal velocity in the wake of the smooth cylinder at all nine measuring lines at different distances

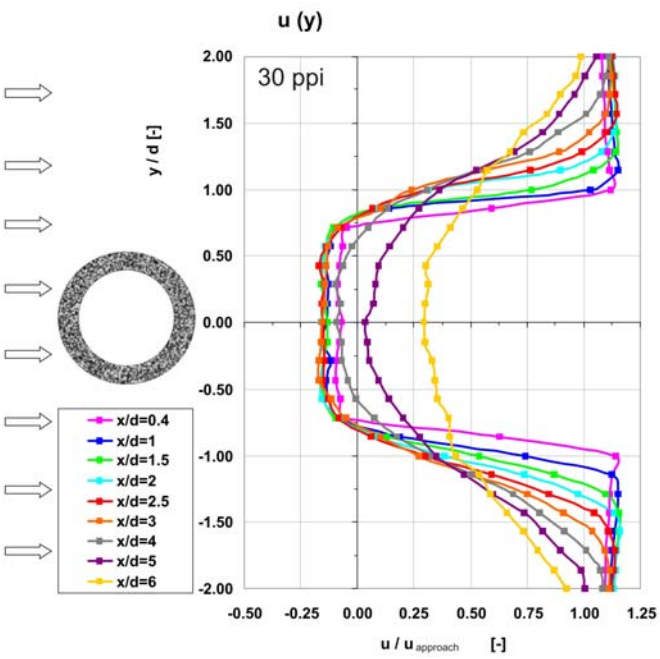

Figure 14 Profiles of horizontal velocity in the wake of a fully porous-coated cylinder at all nine measuring lines at different distances; porosity 30 ppi, porous layer thickness 10 mm

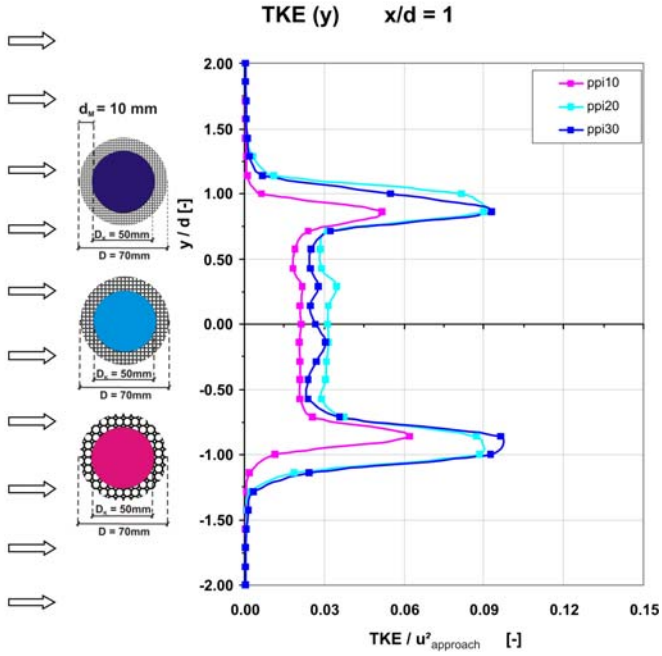

Figure 15 Profiles of turbulent kinetic energy at the measuring line x/d=1 for porous-coated cylinders with layer thickness of 10 mm and varying porosity.

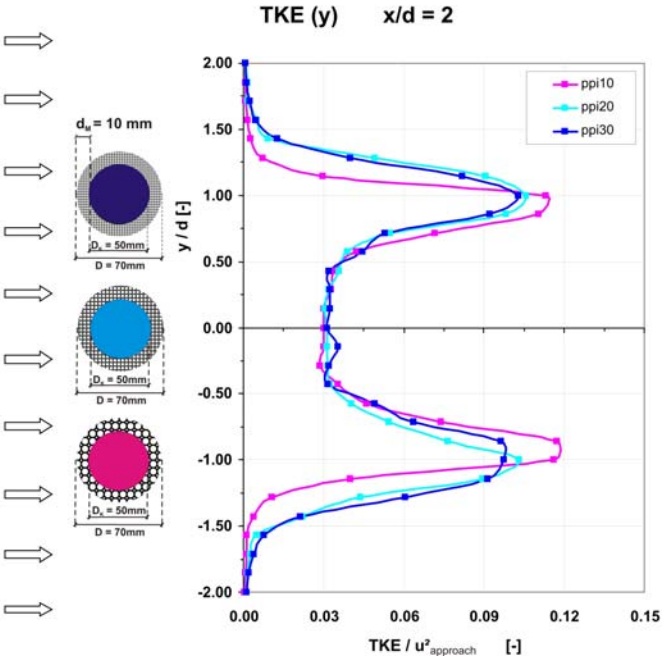

Figure 16 Profiles of turbulent kinetic energy at the measuring line x/d=2 for porous-coated cylinders with layer thickness of 10 mm and varying porosity.

However, the differences in the profiles of TKE at measuring lines further downstream almost vanish as can be seen in Figure 16. This indicates that the porosity of the coating controls the onset of vortex formation. The more porous the coating, the more distant from the cylinder the vortex formation begins.

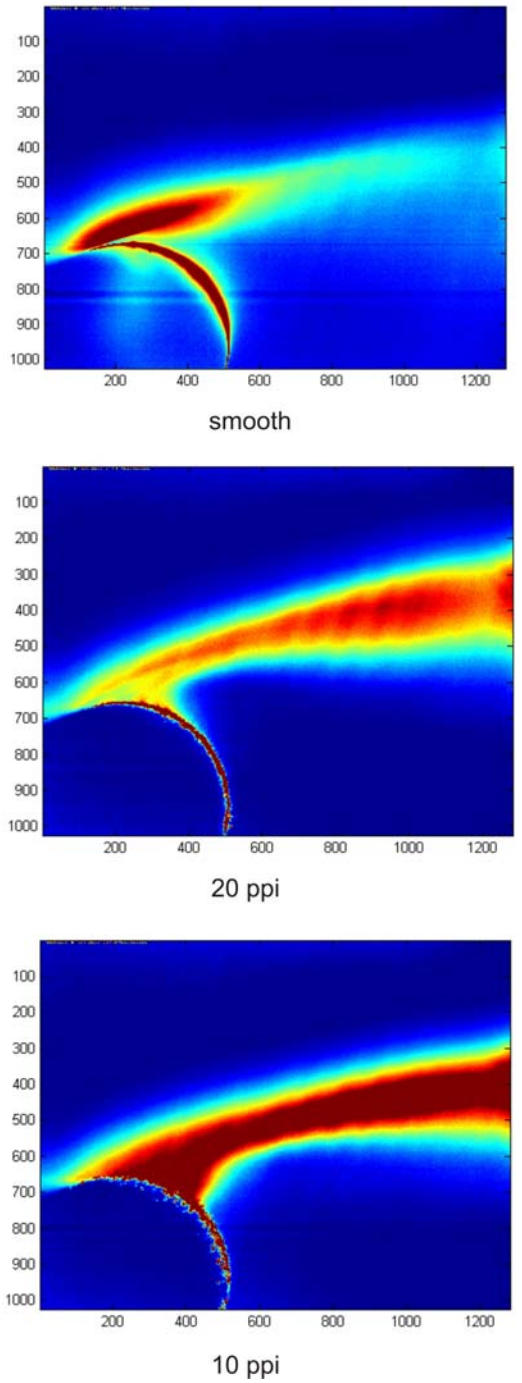

Figure 17 Time-averaged visualization of the free shear layer with different porosities of fully porous-coated cylinders; layer thickness 10 mm, increasing porosity from top to bottom

From flow visualization, see Figure 17, we can infer again that the dimensions of the wake are changed by porous coating. Whereas the region of flow separation is small for the smooth cylinder, this region is increased by porous coating and the free shear layer thickens.

CONCLUSION

The results of the flow analyses have revealed more insight in the fluid mechanics involved. The following list resumes the findings of the investigations, see also Figure 18:

Full porous coating of cylinders has the following fluid mechanical consequences in comparison to a smooth cylinder flow:

- occurrence of momentum cross-exchange between the flowing medium and permeable layer
- leakage on side and rear section of the cylinder (base bleed)
- widening of the wake zone
- reduction of recirculation velocity in the wake
- formation of a thick free shear layer
- increase of base pressure in the separation region
- disappearance of the "drag crisis", i.e. there is no change in the flow field observed over a wide Reynolds number range
- much later development of vortex street downstream of the cylinder
- increase of drag on the windward side
- decrease of drag on the leeward side
- increase of the total resistance of fully porous-coated cylinder

Partial porous coating on the leeward side of cylinders has the following fluid mechanical consequences in comparison to a smooth cylinder flow:

- formation of a thick free shear layer
- reducing the rotational velocity of the recirculating mass in the wake
- increase of base pressure in the separation region
- much later development of vortex street downstream of the cylinder
- no change of drag on the windward side
- decrease of drag on the leeward side
- decrease of the total resistance of leeward porous-coated cylinder

It could be shown experimentally that partial coating by thin porous layers in the lee of a body can lead to drag reduction. It can be conceived as the combination of the positive effects of a smooth surface (lowest surface friction) on the windward side with the positive effects of a permeable wall layer on the lee-ward side (increasing the base pressure in the wake). Thus, it is possible to reduce the total resistance of a body in a flow. This phenomenon could be demonstrated clearly. The drag reduction measured was up to 8% (measured with a balance accuracy < 0.1 %). However, it should be emphasized that all results presented for the leeward coating of cylinders are measured with cylinders having different half-cylinder surface properties,

i.e. the front half was smooth and the rear half was porous-coated. This means that the surface properties change at an angle of 180°. It is most likely that an optimisation of this angle leads to further drag reduction. Additional work on the subject is currently underway and is based on measurements at higher Reynolds numbers, an optimized starting position (angle) of the permeable wall layer and the vibration behaviour of porous-coated cylinders.

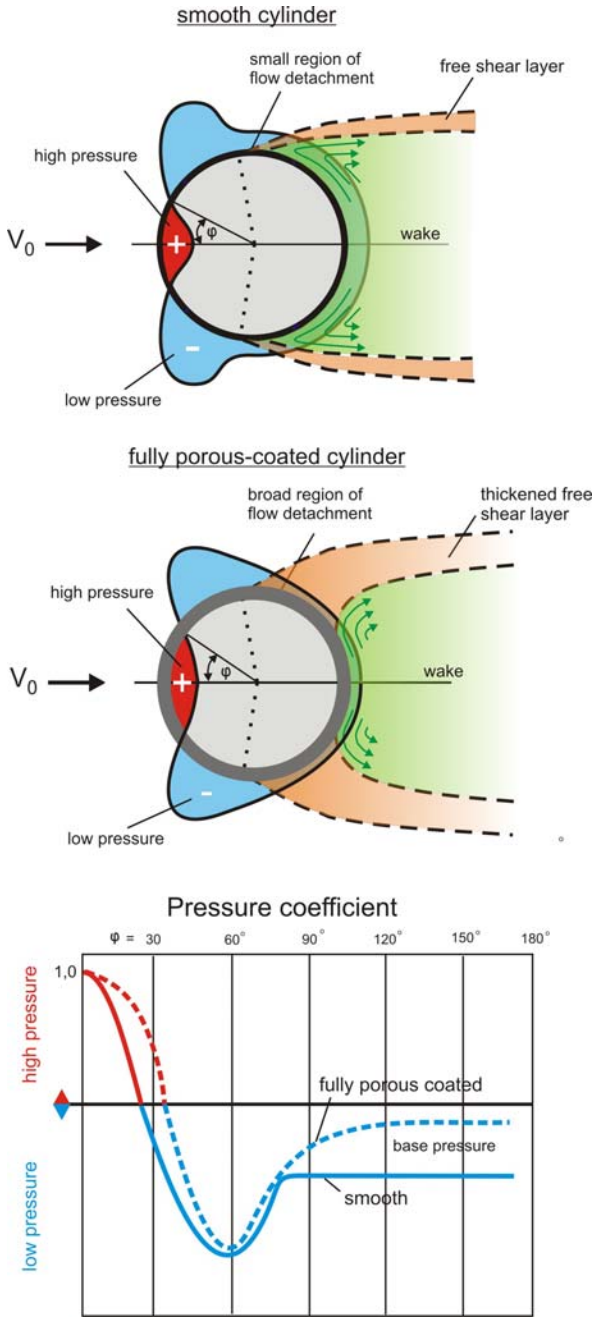

Figure 18 Phenomenology of the flow around porous-coated cylinders

REFERENCES

[1] Darcy, H., Les fontaines publiques de la ville de Dijon, Dijon, 1856, Paris

[2] Bear, J., Dynamics of fluids in Porous Media, Dover Publications, New York, 1972

[3] Forchheimer, P., Lehr- und Handbuch der Hydraulik, 5 Bände, 1914-1916

[4] Breugem, W. P., Boersma, B. J., Uittenbogaard, R. E., The influence of wall permeability on turbulent channel flow, *Journal of Fluid Mechanics*, 562, 2006, S. 35–72

[5] Bruneau, C-H., Mortazavi, I., Flow regularisation and drag reduction around blunt bodies using porous devices , *Proc. European Drag Reduction and Flow Control Meeting*, Ischia, Italy, 2006

[6] Bruneau, C-H., Mortazavi, I., Control of vortex shedding around a pipe section using a porous sheath", *International Journal of Offshore and Polar Engineering*, 16, Nr. 2, 2006 b, S. 90–96

[7] Bhattascharyya, S. , Singh, A. K., Reduction of drag and vortex shedding frequency through porous sheath around a circular cylinder, *Int. Journal for numerical methods in fluids,* 65, 2011, S. 683–698

[8] Strouhal, V., Über eine besondere Art der Tonerregung, *Annalen der Physik und Chemie,* 5 (10), 1878, pp. 216–251

[9] Kármán v., T., Über den Mechanismus des Widerstandes, den ein bewegter Körper in einer Flüssigkeit erfährt, *Nachrichten d. K. Gesellschaft d. Wissenschaften zu Göttingen*. Math.-phys. Kl. 1911, pp. 509-517 und Kl. 1912 pp.547-556

[10] Wieselsberger, C., Neuere Feststellungen über die Gesetze des Flüssigkeits- und Luftwiderstandes, *Physikalische Zeitschrift*, Nr. 11, 1921, S. 321-328

[11] Roshko, A., Experiments on the flow past a circular cylinder at very high Reynolds number, *Journal of Fluid Mechanics*, 10, 1961, 345-356

[12] Hoerner, S.F., Fluid-Dynamic Drag, Selbstverlag; New Jersey, 1965

[13] Zdravkovich, M.M., Flow around circular cylinders, Vol.1: Fundamentals, Oxford University Press, 1997

[14] Zdravkovich, M.M., Flow around circular cylinders, Vol.2: Applications, Oxford University Press, 2003

[15] Fage, A., Warsap, J. H., The effects of turbulence and surface roughness on the drag of a circular cylinder, Aero. Res. Comm. R. & M. No. 1283, 1929

[16] Achenbach, E., Distribution of local pressure and skin friction around a circular cylinder in cross-flow up to Re = 5x10e6, *Journal of Fluid Mechanics*, 34, 1968, 625-639

[17] Achenbach, E., Influence of surface roughness on the cross-flow around a circular cylinder, *Journal of Fluid Mechanics* 46, Nr. 2, 1971, S. 321–335

[18] Achenbach, E. and Heinecke, E., On Vortex Shedding From Smooth and Rough Cylinders in the Reynolds Numbers from 6x10e3 to 5x10e6, *Journal of Fluid Mechanics*, 109, 1981, 239-251

[19] Nikuradse, J., Strömungsgesetze in rauhen Rohren, Forschungsheft 361, Teil B, VDI Verlag, Berlin, 1933

[20] Price, P., Suppression of the fluid induced vibration of circular cylinders, *J. Engr. Mech.* Div. Am. Soc. Civ. Engrs. 82, 1956, Paper 1030

[21] Wong, H.Y., A means of controlling bluff body separation, *J. Ind. Aerodyn.*, 4, 1979, 183 -201

[22] Galbraith, R.A.McD., Flow pattern around a shrouded cylinder at Re=5 x 10^3, *Journal of Wind Engineering and Industrial Aerodynamics*, 6, 1980, 227-242